Circuits Syst Signal Process (2015) 34:1461–1480
DOI 10.1007/s00034-014-9925-z

Fractional Order Sallen–Key and KHN Filters: Stability and Poles Allocation

Ahmed Soltan · Ahmed G. Radwan · Ahmed M. Soliman

Received: 4 June 2014 / Revised: 20 October 2014 / Accepted: 21 October 2014 /
Published online: 13 November 2014

Abstract This paper presents the analysis for allocating the system poles and hence controlling the system stability for KHN and Sallen–Key fractional order filters. The stability analysis and stability contours for two different fractional order transfer functions with two different fractional order elements are presented. The effect of the transfer function parameters on the singularities of the system is demonstrated where the number of poles becomes dependent on the transfer function parameters as well as the fractional orders. Numerical, circuit simulation, and experimental work are used in the design to test the proposed stability contours.

Keywords Stability, LTI system · Fractional-order system · Filters · Oscillators · Control

1 Introduction

The theory of fractional differential equations has attracted increasing attention in the past few years [2,24,26,28]. Facts show that many systems can be described with the

A. Soltan
School of Electrical and Electronic Engineering, Newcastle University, Newcastle upon Tyne, UK
e-mail: a.s.a.abd-el-aal@newcastle.ac.uk

A. G. Radwan (✉)
Department of Engineering Mathematics and Physics, Cairo University, Cairo, Egypt
e-mail: agradwan@ieee.org

A. G. Radwan
Nanoelectronics Integrated Systems Center (NISC), Nile University, Giza, Egypt

A. M. Soliman
Department of Electronics and Communications Engineering, Cairo University, Cairo, Egypt
e-mail: asoliman@ieee.org

help of fractional derivatives in interdisciplinary fields, for example, electromagnetic waves [34], viscoelastic systems [36,44]. Furthermore, applications of fractional calculus have been reported in many areas such as physics [3,8], engineering [6,17,27], stability analysis [13,21,22,29,32,35], circuit design [11,30,31,33,39,40], and mathematical biology [45]. A general fractional-order system can be described by a transfer function of incommensurate real orders of the following form:

$$T(s) = \frac{b_{K+1}s^{\beta_K} + \cdots + b_1 s^{\beta_0} + b_0}{a_{m+1}s^{\alpha_m} + \cdots + a_1 s^{\alpha_0} + a_0} = \frac{N(s)}{D(s)}, \tag{1}$$

where $a_r\,(r = 0, 1, 2, \ldots m+1)$, and $b_i\,(i = 0, 1, 2, \ldots K+1)$ are constants, and α_m and β_K are arbitrary real numbers and without loss of generality they can be arranged as $\alpha_m > \alpha_{m-1} > \alpha_{m-2} > \ldots \alpha_0$, and $\beta_m > \beta_{m-1} > \beta_{m-2} > \ldots \beta_0$ and $\beta_K \leq \alpha_m$. In case of filters, the magnitude response at ω approaches 0 and ∞ is equal to $\frac{b_0}{a_0}$ and $\frac{b_{K+1}}{a_{m+1}}$, respectively, which determine the type of this filter.

Generally, there are two methods to study the stability of any system; the first one studies stability in the time domain and the other in the frequency domain. For the time domain analysis, numerous reports have been published on this matter, with particular emphasis on the application of Lyapunov's second method, or on using the idea of matrix measure [15,19,21]. On the other hand, the second approach depends on studying the stability of systems with arbitrary order in the frequency domain [6, 9,29,32,35]. Accordingly, there is no closed form for the line that separates the stable and unstable regions for the common systems especially the second order system. This line is called the stability contour during this work.

Conventionally, many practical systems like the mass spring system [6], PID systems [9,15,20,23], and electronic circuits [8,33,43] are represented by a second order transfer function. Therefore, this paper aims to drive a stability contours not only for the conventional second order systems but also for the fractional order systems with two different fractional order elements. Due to the different fractional orders (α, β), there are two types of the characteristic equations for a system with two different fractional orders; the general form of characteristic equation which can be written as follows: $(s^{\alpha+\beta} + as^{\alpha} + bs^{\beta} + c)$ and the special case when b or $a = 0$. Consequently, the stability analysis and a closed form of the stability contours for both forms of the characteristic equations are discussed. Also, the effect of the fractional orders and the transfer function parameters on the number of poles and their locations is discussed.

Consequently, this paper is organized as follows: the concept of stability analysis is presented in Sect. 2. The effect of the transfer function parameters on the system singularities is discussed in Sect. 3. After that, the stability analysis of KHN and Sallen–Key filters is illustrated in Sects. 4 and 5, respectively. Finally, the conclusion of this work is summarized in Sect. 6.

2 Concept of Stability Analysis

Fractional systems, or non-integer order systems, can be considered as a generalization of integer order systems. Then from (1), the characteristic equation of a gen-

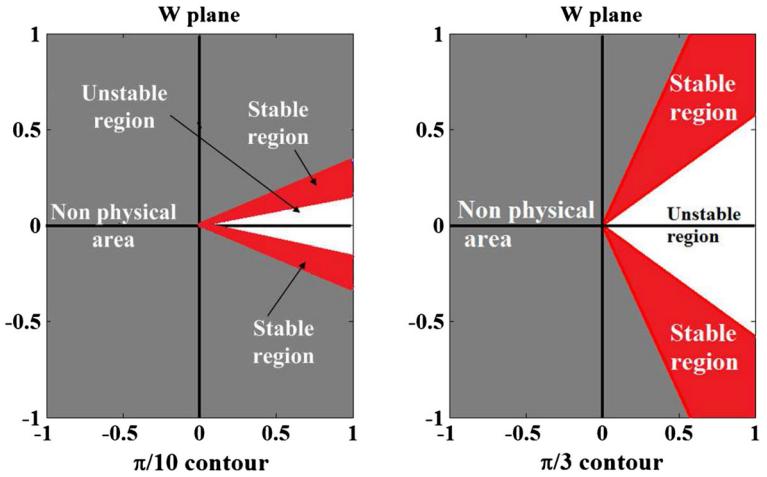

Fig. 1 Stability contour for different values of α

eral fractional order linear time invariant (FLTI) system can be given by (2) for $\alpha_i = k_i/v$.

$$D(s) = a_m s^{\alpha_m} + \cdots + a_1 s^{\alpha_1} + a_0 s^{\alpha_0} = \sum_{i=0}^{m} a_i s^{\frac{k_i}{v}}, \tag{2}$$

where k_i and v are constant integers. By using the technique in [6,7,35], the characteristic equation of (2) can be written in the W-plane($W = s^{1/v}$) as follows:

$$D(W) = a_m W^{k_m} + \cdots + a_1 W^{k_1} + a_0 W^{k_0} = \sum_{i=0}^{m} a_i W^{k_i}, \tag{3}$$

which is a polynomial in W, then the roots of this equation can be easily obtained based on the coefficients a_i and the powers k_i. Generally, these m roots are distributed in the W-plane; however, the conventional s-plane which is based on the principal sheet of the Riemann surface and defined by $-\pi < \angle s < \pi$ where its corresponding region in the W-domain is defined by $-\pi/v < \angle W < \pi/v$. Moreover, the W-plane region corresponding to the right half s-plane is defined by$-\pi/2v < \angle W < \pi/2v$ which reflect the unstable physical poles [35]. The Remaining W-plan which is defined by$|\angle W| > \pi/v$ is not physical which means that any pole in that region will not have a corresponding physical pole in the conventional s-plane. Therefore, the corresponding physical s-plane is mapped into a section in the W-plane, and this section based on the value of v as shown from Fig.1 where two different contours are depicted at $v = 3$ and $v = 10$. The white and red sections represent the unstable and stable physical s-plane, while the gray section represents the nonphysical or secondary Riemann sheets.

On the other hand, the system is stable in the time domain if it is a bounded input bounded output (BIBO) system. So, finite time singularities occur when the

output variable increases toward infinite at a finite time at certain input in the time domain [2,6]. Just as the exponential naturally arises out of the solution to integer order differential equations, the Mittag-Leffler function plays an analogous role in the solution of non-integer order differential equations [16]. In fact, the exponential function itself is a very specific form, one of an infinite set, of this seemingly ubiquitous function. The standard definition of the Mittag-Leffler is given by

$$E_{\alpha,\beta}(z) = \sum_{k=0}^{\infty} \frac{z^k}{\Gamma(\alpha k + \beta)}, \alpha > 0, \beta > 0. \tag{4}$$

This generalized function will tend to the exponential function as $\alpha = \beta = 1$. By applying the partial fractional concept on the transfer function in (1) and using the inverse laplace transform using the fact that $L(t^{\beta-1}E_{\alpha,\beta}(\lambda t^{\alpha})) = \frac{s^{\alpha-\beta}}{(s^{\alpha}-\lambda)}$, the time domain responses can be obtained. The asymptotic behavior of Mittag-Leffler functions plays a very important role in the interpretation of the solution of various problem. The asymptotic expansion of $E_{\alpha,\beta}(z)$ is based on the integral representation of the Mittag-Leffler function in the form:

$$E_{\alpha,\beta}(z) = \frac{1}{2\pi i}\int_{\Omega} \frac{t^{\alpha-\beta}\exp(t)}{t^{\alpha}-z}\mathrm{d}t, \Re(\alpha) > 0, \Re(\beta) > 0, z, \alpha, \beta \in C, \tag{5}$$

where the path of integration Ω is a loop starting and ending at $-\infty$ and encircling the circular disk $|t| \leq |z|^{1/\alpha}$ in the positive sense, $|\arg t| < \pi$ on Ω. The integral representation (5) can be used to obtain the asymptotic expansion of the Mittag-Leffler function at infinity [4,25]. In case of the systems with two fractional order elements, the value of α is limited as $0 \leq \alpha \leq 2$. Accordingly, the Mittag-Leffler function has asymptotic estimates, for example, when $0 < \alpha < 2$ and μ is a real number where $\frac{\alpha\pi}{2} < \mu < \min[\pi, \alpha\pi]$, then there holds the following asymptotic expansion [16]:

$$E_{\alpha,\beta}(z) = \frac{1}{\alpha} z^{\frac{1-\beta}{\alpha}} \exp(z^{1/\alpha}) - \sum_{r=1}^{N^*} \frac{1}{\Gamma(\beta-\alpha r)} \frac{1}{z^r} + O\left[\frac{1}{z^{N^*+1}}\right] \tag{6}$$

as $|z| \to \infty$, $|\arg z| \leq \mu$ and

$$E_{\alpha,\beta}(z) = -\sum_{r=1}^{N^*} \frac{1}{\Gamma(\beta-\alpha r)} \frac{1}{z^r} + O\left[\frac{1}{z^{N^*+1}}\right], \tag{7}$$

as $|z| \to \infty$, $\mu \leq |\arg z| \leq \pi$

3 System Singularities

The transfer function of the fractional order system with two different fractional order elements is given by

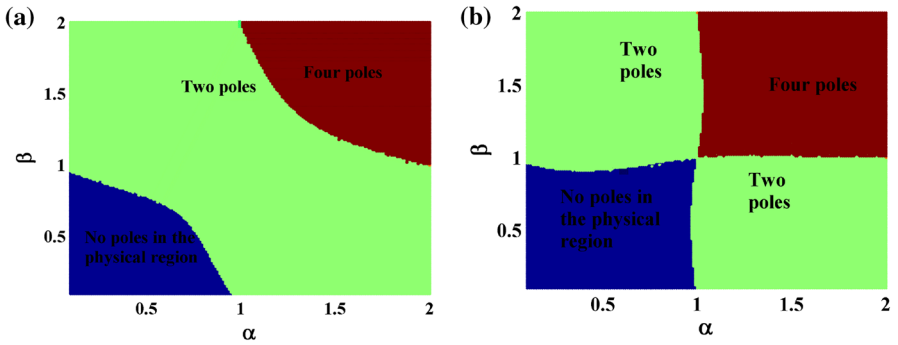

Fig. 2 Change in the number of system poles with respect to α and β when **a** $a = b = 1$, **b** $a = 10, b = 10$

$$T(s) = \frac{N(s)}{s^{\alpha+\beta} + as^{\alpha} + b}. \tag{8}$$

Generally, the system singularities are represented by the denominator and control the system stability. Hence, the singularities of (8) are obtained by solving the following polynomial:

$$s^{\alpha+\beta} + as^{\alpha} + b = 0. \tag{9}$$

To calculate the roots of the polynomial of (9), let $s = \sigma \pm j\omega = s_1 e^{\pm j\theta}$. Therefore, the polynomial of (9) could be rewritten as follows:

$$s_1^{\alpha+\beta} \mathrm{e}^{j(\alpha+\beta)\theta} + as_1^{\alpha} \mathrm{e}^{j\alpha\theta} + b = 0. \tag{10}$$

For the traditional systems ($\alpha = \beta = 1$), there are always two poles. Yet, for the fractional orders system, the number of singularities depends on the fractional orders (α, β) and the transfer function parameters $\{a, b\}$ as shown in Fig. 2a, b for the two different cases of $(a, b) = (1, 1)$ and $(10, 10)$, respectively. In addition, the fractional order system singularities discussed here belong to the essential-type singularities [10,14]. There are three cases for the number of physical poles in the s-plane of the fractional order system as follows: no poles in the physical s-plane, two, and four poles in the physical s-plane as shown in Fig. 2. Thus, the fractional order system singularities are function of $\{\alpha + \beta, \alpha, a, b\}$. This means, the system can be designed for a specified singularities, although the number of the fractional order elements is constant which adds more design degree of freedom to the system design.

By equating the real and imaginary parts of (10) to zero and using simple trigonometric relations, the poles of the system are given by

$$s_1 = \left(\frac{-a\sin(\alpha\theta)}{\sin((\alpha+\beta)\theta)}\right)^{1/\beta} = \left(\frac{-b\sin((\alpha+\beta)\theta)}{a\sin(\beta\theta)}\right)^{1/\alpha}. \tag{11}$$

From (11), the value of θ is a function of the fractional orders (α, β) and the parameters (a, b) thus increasing the design degree of freedom. By solving (11) numerically for θ

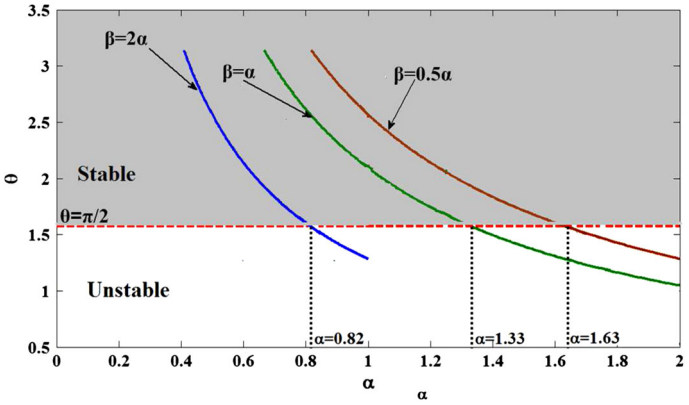

Fig. 3 Change of θ with respect to α different values of β for $a = b = 1$

with respect to α, the system has a solution for θ if there are singularities in the physical region in the W-plane equivalent to the traditional s-plane. On the other hand, the system has no solutions for θ if no singularities exist in the physical s-plane as shown in Fig. 3, and this means the system is unconditionally stable in this case. Furthermore, the system could be solved to allocate the poles at certain points in the s-plane. For example, when $\beta = \{2\alpha, \alpha, 0.5\alpha\}$, the system is stable for $\alpha \leq \{0.82, 1.33, 1.63\}$, respectively, where all the values of θ are greater than $\pi/2$ as illustrated in Fig. 3.

Using (11), to design the system for certain poles (phase (θ) , magnitude (s_1) , and number of poles), the transfer function parameters $\{a, b\}$ could be written as follows:

$$a = s_1^{\alpha} \frac{\sin((\alpha+\beta)\theta)}{\sin(\alpha\theta)}, \tag{12a}$$

$$b = s_1^{\alpha+\beta} \frac{\sin(\beta\theta)}{\sin(\alpha\theta)}. \tag{12b}$$

From (12), the values of the parameters a and b tend toward infinity at $\alpha\theta = \pi$ as shown in Fig. 4c.

However, for $\alpha + \beta < 1$, the system variables a and b always have a value for each value of θ but in this case, the value of a(or b) must be negative to have a pole as shown in Fig. 4a, b. For example, to obtain system poles with $(s_1, \theta) = (2, 0.4\pi)$ at $(\alpha, \beta) = (0.8, 1.2)$ and $(1.6, 1.8)$, the value of the transfer function parameters is $(a, b) = (-1.6, 4.7)$ and $(3.485, 9)$, respectively. Yet, in the traditional case ($\alpha = \beta = 1$), there is only one solution for the system parameters $(a, b) = (1.2361, 4)$ that satisfies the required system poles $((s_1, \theta) = (2, 0.4\pi))$. So, for the fractional order system, there is an infinite number of solutions which achieve the required system response as shown in Fig.4d.

Finally, the singularity analysis presented in this section can be generalized for the general form of the characteristic equation. So, the same relations are obtained for the system parameters and the singularities for the characteristic equation $s^{\alpha+\beta} + as^{\alpha} + bs^{\beta} + c$ using the same analysis steps presented in this section. Although the number

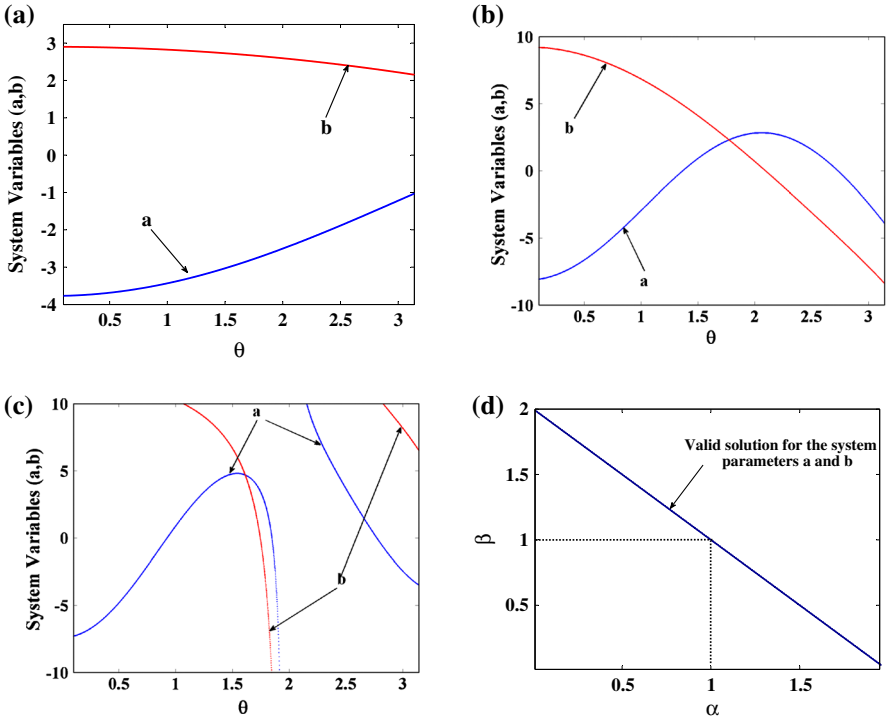

Fig. 4 Change of a and b with respect to θ when $s_1 = 2$ **a** $(\alpha, \beta) = (0.3, 0.5)$ **b** $(\alpha, \beta) = (0.8, 1.2)$, **c** $(\alpha, \beta) = (1.6, 1.8)$, and **d** Available solutions for the system parameters with change in α and β at $\theta = 0.4\pi$ and $s_1 = 2$

of the fractional order elements is the same, the system degree of freedom is increased by one in this case.

4 KHN Filter Stability

KHN is one of the important filter circuits because it introduces low-pass, band-pass, and high-pass responses simultaneously. The general form of the KHN filter transfer function is given in (13). The relations between $N(s)$ and the circuit elements are summarized in Table 1 for the three responses. In addition, the characteristic equation of the three responses is the same which means the stability analysis is the same for the three responses. The circuit diagram of the fractional order KHN filter is depicted in Fig. 5. Another advantage of the KHN filter is that its transfer function presented in (13) is similar to the transfer function of many of the systems that have two fractional elements. Hence, the following analysis could be applied to these systems.

$$\frac{V_1}{V_{in}} = \frac{N(s)}{s^{\alpha+\beta} + \frac{R_3}{R_1 C_1}\frac{(R_5/R_6)}{R_3+R_4}s^{\alpha} + \frac{R_5/R_6}{C_1 C_2 R_1 R_2}}. \tag{13}$$

Table 1 Summary of the relations between the circuit elements and the transfer function parameters

Parameter	Relation		
	FLPF	FBPF	FHPF
$N(s)$	$\frac{R_5/R_6}{C_1C_2R_1R_2}\frac{R_4}{R_3+R_4}$	$s^{\alpha}\frac{1}{C_1R_1}\frac{R_5/R_6}{C_1C_2R_1R_2}\frac{R_4}{R_3+R_4}$	$s^{\alpha+\beta}\frac{R_5/R_6}{C_1C_2R_1R_2}\frac{R_4}{R_3+R_4}$
a	$\frac{R_3}{R_1C_1}\frac{(R_5/R_6)}{R_3+R_4}$	$\frac{R_3}{R_1C_1}\frac{(R_5/R_6)}{R_3+R_4}$	$\frac{R_3}{R_1C_1}\frac{(R_5/R_6)}{R_3+R_4}$
b	$\frac{R_5/R_6}{C_1C_2R_1R_2}$	$\frac{R_5/R_6}{C_1C_2R_1R_2}$	$\frac{R_5/R_6}{C_1C_2R_1R_2}$

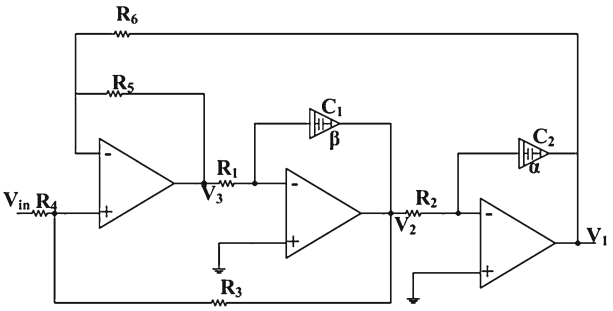

Fig. 5 Fractional order KHN filter

Although the design and analysis of the fractional order KHN filter have been presented before [1,12,42,43], the stability analysis of these filters was not presented. So, this section focuses on the stability analysis of the KHN filters. As the transfer function of (13) is the same as the transfer function of (8), the equation of (8) will be used in the following analysis, and then the relations tabulated in Table 1 are used to calculate the circuit elements value. So, the condition of stability for the traditional fractional order system is obtained by substituting $\theta = \pi/2$ in (11) which represents the boundary line $s = \pm j\omega$ as follows.

$$\left(\frac{-a\sin(0.5\alpha\pi)}{\sin(0.5(\alpha+\beta)\pi)}\right)^{\alpha} = \left(\frac{-b\sin(0.5(\alpha+\beta)\pi)}{a\sin(0.5\beta\pi)}\right)^{\beta}, \alpha+\beta \neq 2, \tag{14a}$$

$$\omega_o = \left(\frac{-a\sin(0.5\alpha\pi)}{\sin(0.5(\alpha+\beta)\pi)}\right)^{1/\beta} = \left(\frac{-b\sin(0.5(\alpha+\beta)\pi)}{a\sin(0.5\beta\pi)}\right)^{1/\alpha}, \alpha+\beta \neq 2. \tag{14b}$$

Consequently, the system stability is dependent on the parameters $\{\alpha, \beta, a, b\}$ which means extra degree of freedom. So, the stability condition of (14a) can be used to draw a stability contour for the filter at different combinations of the equation parameters. From (14b), for ω_o to be real positive at $\alpha+\beta > 2$, the value of a must be positive ($a > 0$) and $b/a > 0$. On the contrary, when $\alpha+\beta < 2$, it should be $a < 0$ and $b/a < 0$ for the value of ω_o to be a real positive value as shown in Fig. 6. In addition, for $\alpha+\beta > 1$, the value of b must be positive for the system to be stable. On the other hand, the stability contours in the $\alpha-\beta$ plane using (14) are illustrated in Fig. 7 at different values of the transfer function parameters a and b. The region under

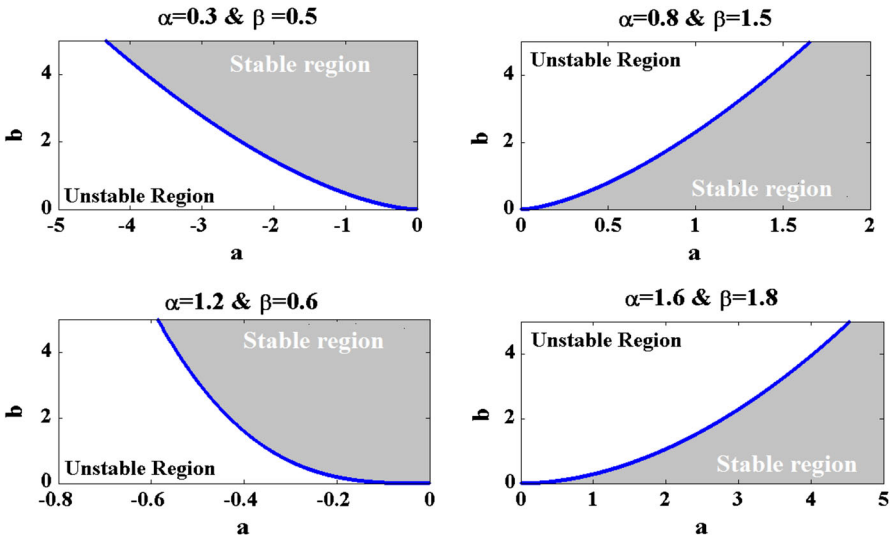

Fig. 6 Stability contours for the transfer function of (8) at different values of (α, β)

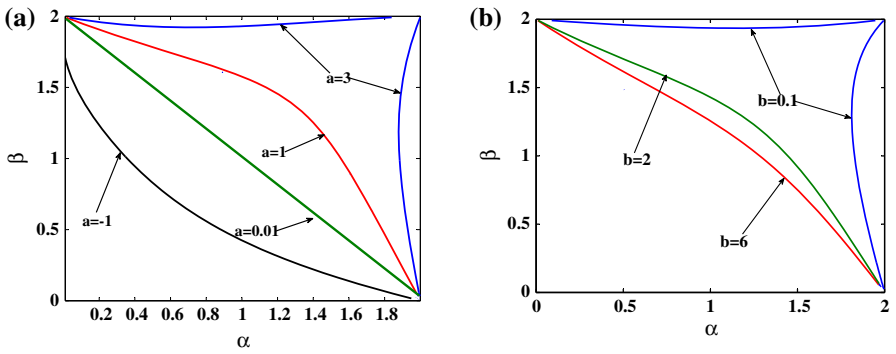

Fig. 7 System stability contour in the $\alpha - \beta$ plane, **a** for different values of a and when $b = 1$, and **b** for different values of b and when $a = 1$

the contour line represents the combination of the fractional orders α and β which produces a stable system at the given value of a and b. Indeed, as the values of α and β become close to the contour lines, the damping in the system increases as the system singularities become closer to the imaginary axis. When a tends to zero, the stability curve will be close to the straight line $(\alpha + \beta = 2)$ where the area under this line is stable and above it is unstable as depicted in Fig. 7a for $a = 0.01$. Yet, as the parameter a increases, the stability contour line starts to take a curvature shape and the area under the line increases. Then, the stable area increases with the increase in the parameters a. On the contrary, the increase in the transfer function parameter b reduces the stable region as shown in Fig. 7b.

Obviously, system singularities are considered a vital factor for measuring the system stability. Hence, it is necessary to present the relation between the previous

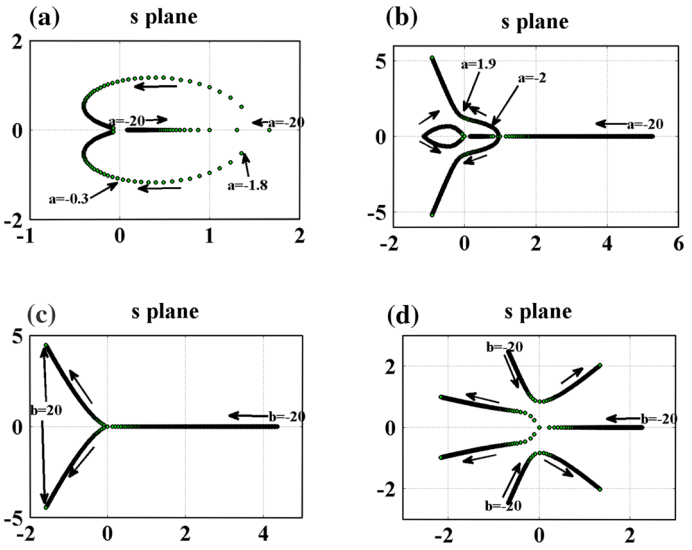

Fig. 8 Movement of the system singularities with respect to a and b, **a** for $b = 1, \alpha = 1.2$, and $\beta = 0.6$, **b** for $b = 1, \alpha = 1.6$, and $\beta = 1.8$, **c** for $a = 1, \alpha = 1.2$, and $\beta = 0.6$, and **d** for $a = 1, \alpha = 1.6$, and $\beta = 1.8$

analysis and the system singularities to verify the analysis. Consequently, the study of the system singularity movement due to the transfer function parameters $\{a, b, \alpha, \beta\}$ is illustrated in Fig. 8. For small values of a, the system starts unstable and then the singularities move toward the stable region as the value of the parameter a increases as shown in Fig. 8a, b. This is the same result obtained before from the stability contours of Fig. 7a. On the other hand, the system is unstable for $b < 0$ as mentioned before in Fig 6. Yet, for $b \geq 0$, the system starts stable and moves toward the unstable region as b increases as depicted in Fig. 8c, d. Accordingly, the singularities movement due to the system parameters matches with the proposed stability contour analysis. Then, these stability contours provide an easy and fast way to determine the system stability. In addition, the number of poles is also dependent on the parameters a and b as summarized in Table 2 which confirms the results discussed before.

The frequency response of the KHN filter using ADS is presented in Fig. 9 at different fractional orders for $a = b = 1$. As the point $(\alpha, \beta) = (1.2, 1.5)$ is very close to the stability contour (from Fig 7a), the damping in the filter response is very large as expected. On the other hand, the points $(\alpha, \beta) = (0.7, 0.7)$ and $(0.8, 1.3)$ are far from the stability contour and this makes their frequency response to have a very small damping as depicted in Fig. 9.

5 Sallen–Key Filter Stability

Sallen–Key (SK) filters are considered one of the most common and well-known filter family [37,38]. The conventional Sallen–Key family provides a second order filters by using two integer order capacitors and one op-amp. Although the design and analysis

Table 2 Summary of the stability analysis in the s-plane

(α, β)	a	b	Number of poles	Stable/unstable
(1.2, 0.6)	$-20 \le a < -0.3$	1	2	Unstable
	$a \ge -0.3$	1	2	Stable
(1.6, 1.8)	$-20 \le a \le -1.3$	1	2	Unstable
	$-1.3 < a \le 1.9$	1	4	Unstable
	$a > 1.9$	1	4	Stable
(1.2, 0.6)	1	$b < 0$	1	Unstable
	1	$b \ge 0$	2	stable
(1.6, 1.8)	1	$b < 0$	3	Unstable
	1	$0 \ge b \le 0.2$	4	Stable
	1	$b > 0.2$	4	Unstable

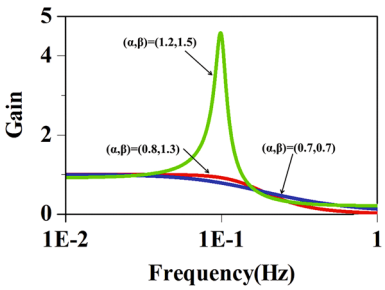

Fig. 9 KHN frequency response at $a = b = 1$

of the fractional order Sallen–Key filter were introduced before in [41], the stability analysis was not discussed in detail. Therefore, this work studies the Sallen–Key filter stability using two different fractional order elements of different orders (α, β). The transfer function of the fractional order Sallen–Key filter illustrated in Fig. 10 is given as follows:

$$\frac{V_{\text{out}}}{V_{\text{in}}} = \frac{\frac{1}{C_1 C_2 R_1 R_2}}{s^{\alpha+\beta} + \frac{1-R_4/R_3}{R_2 C_2} s^{\alpha} + \left(\frac{1}{R_2 C_1} + \frac{1}{R_1 C_1}\right) s^{\beta} + \frac{1}{C_1 C_2 R_1 R_2}}. \tag{15}$$

To simplify the analysis, the transfer function of (15) can be rewritten as follows:

$$T(s) = \frac{N(s)}{s^{\alpha+\beta} + as^{\alpha} + bs^{\beta} + c}, \tag{16}$$

where $a, b, and c$ are constants and α and β are the fractional orders and $0 < \alpha, \beta \le 2$. The relation between the transfer function parameters and the circuit elements is summarized in Table 3. Basically, the transfer function of (16) is the general form of the transfer function of fractional order system with two different fractional order elements. So, for the special case of $a = 0$ or $b = 0$, the transfer function of (16) returns to the form of (8) and hence the filter stability is controlled by the relation

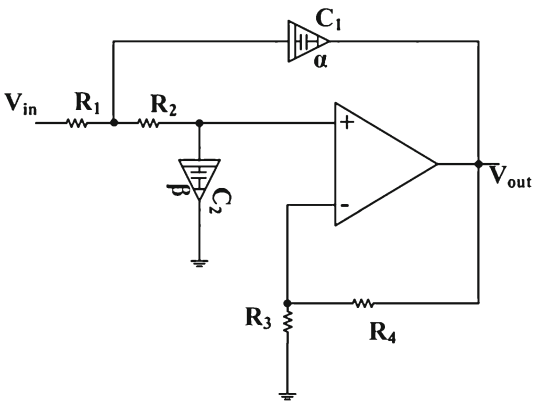

Fig. 10 Fractional order Sallen–Key filter

Table 3 Relations between the SK circuit elements and the transfer function parameters

Parameter	Relation
$N(s)$	$\frac{1}{C_1C_2R_1R_2}$
a	$\frac{1-R_4/R_3}{R_2C_2}$
b	$\frac{1}{R_2C_1}+\frac{1}{R_1C_1}$
c	$\frac{1}{C_1C_2R_1R_2}$

of (14). Indeed, this form of the transfer function results from the existence of the subtraction term in the dominator of the traditional transfer function ($\alpha = \beta = 1$). By equating the real and imaginary parts of the characteristic equation of (16) to zero, the condition of stability for the fractional order system is obtained by solving the following equations:

$$\omega^{\alpha+\beta}\sin(0.5(\alpha+\beta)\pi) + a\omega^{\alpha}\sin(0.5\alpha\pi) + b\omega^{\beta}\sin(0.5\beta\pi) = 0, \tag{17a}$$

$$\omega^{\alpha+\beta}\cos(0.5(\alpha+\beta)\pi) + a\omega^{\alpha}\cos(0.5\alpha\pi) + b\omega^{\beta}\cos(0.5\beta\pi) + c = 0. \tag{17b}$$

From (17), the stability condition becomes dependent on the parameters $\{\alpha, \beta, a, b, c\}$ instead of the parameters $\{a, c\}$ for the traditional systems. Consequently, this increases the design degree of freedom. Thus, for each combination of the transfer function parameters $\{\alpha, \beta, a, b, c\}$, there is a different stability contour. To illustrate the stability analysis of (17), two special cases are discussed in the following subsections.

5.1 Equal Order Systems

This section considers stability for the fractional order system with fractional order elements of the same order $\alpha = \beta$. So, the stability condition of (17) can be rewritten as follows:

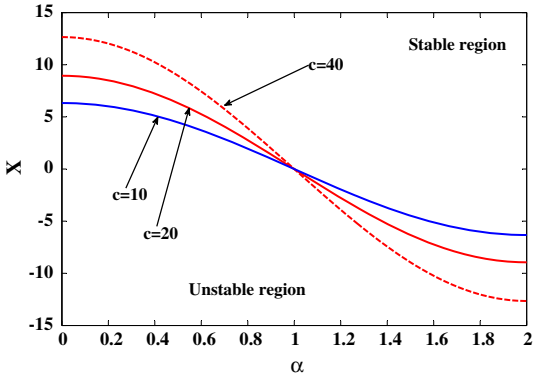

Fig. 11 Stability contour of the fractional order system at different values of c

$$\omega^{2\alpha}\cos(\alpha\pi) + (a+b)\omega^{\alpha}\cos(0.5\alpha\pi) + c = 0, \tag{18a}$$

$$\omega^{\alpha}\sin(\alpha\pi) + (a+b)\sin(0.5\alpha\pi) = 0. \tag{18b}$$

Then, for $X = a + b$ and making some simplifications, the stability condition for this case can be determined by

$$X = \pm 2\sqrt{c\cos(0.5\alpha\pi)}. \tag{19}$$

For the value of X to be a real value, the value of c must be greater than zero which means the system cannot be designed for $c < 0$ in this case. The stability contour of the fractional order system in this case is illustrated in Fig. 11 for different values of c. The interesting result here is that the parameter X takes positive or negative values and the system remains in the stable region, which means the system can be designed for negative values of X. This increases the design flexibility.

5.2 Fractional Order System of Dependent Orders

In the following analysis of the fractional order system stability, the fractional orders α and β are dependent by a factor k where $0 < \alpha$, $k\alpha \leq 2$. Then, under these conditions, the transfer function of (16) can be written as follows:

$$T(s) = \frac{N(s)}{s^{\alpha(1+k)} + as^{\alpha} + bs^{k\alpha} + c}. \tag{20}$$

By equating the real and imaginary parts of the characteristic equation of (20), the stability condition can be calculated from the following relations.

$$\omega^{\alpha(1+k)}\cos(0.5\alpha(1+k)\pi) + a\omega^{\alpha}\cos(0.5\alpha\pi) + b\omega^{\alpha k}\cos(0.5\alpha k\pi) + c = 0, \tag{21a}$$

$$\omega^{\alpha(1+k)}\sin(0.5\alpha(1+k)\pi) + a\omega^{\alpha}\sin(0.5\alpha\pi) + b\omega^{\alpha k}\sin(0.5\alpha k\pi) = 0. \tag{21b}$$

By solving (21a, b) together, the stability contour for the transfer function of (20) is obtained. To demonstrate the effect of the transfer function parameters on the system stability, a special case for $k = 2$ is studied in the following analysis. So for $k = 2$, the oscillation frequency and the condition of oscillation are given by

$$\omega_{\text{osc}} = \frac{\cos(0.5\alpha\pi)}{4(\cos(0.5\alpha\pi))^2 - 1}\Big[-b \pm \sqrt{(b^2 - a(4 - (\sec(0.5\alpha\pi))^2))}\Big]^{1/\alpha}, \tag{22a}$$

$$\omega_{\text{osc}}^{3\alpha}\cos(1.5\alpha\pi) + b\omega_{\text{osc}}^{2\alpha}\cos(\alpha\pi) + a\omega_{\text{osc}}^{\alpha}\cos(0.5\alpha\pi) + c = 0. \tag{22b}$$

From (22a), the frequency of oscillation ω_{osc} is a function of the parameters $\{a, b, \alpha\}$ which increases the degree of freedom. In addition, the oscillation frequency ω_{osc} is independent on the value of c, and this great advantage can be used to make independent control on the condition of stability and the oscillation frequency. As shown in Fig. 12, the system of (22) has three regions for the oscillation frequency depending on the value a, b, and α. These three regions are as follows: no solution for ω_{osc}, one solution exists for ω_{osc}, and finally two solutions for ω_{osc} exist. Furthermore, the separation between any two regions with the change in the fractional order α occurs always at the same value of α which is called α_c, and from (22a), this value equals $2/3$. The stability contours are also illustrated in Fig. 12 versus the parameters c for the same cases of the parameters a and b. Actually, for $\alpha < \alpha_c$, the filter becomes more stable as the value of c increases. On the contrary, for $\alpha > \alpha_c$, the system moves toward the unstable region as the value of c increases. Although there are two solutions for the oscillation frequency at some cases ($(a, b) = (5, -5)$), there is only one stability contour because one of these values corresponds to a negative value of the parameters c. Thus, the filter in this case is unreliable which means this second contour line is ignored like the dashed line of the stability contour of $(a, b) = (5, -5)$ of Fig. 12. A summary of the relations between the oscillation frequency and the system parameters a, b, and α is shown in Fig. 13. Moreover, the parameter a has a similar effect on the oscillation frequency. Hence, there is a critical value of a which represents the border line between the two regions mentioned before for the oscillation frequency (no solution and two solutions exist), and this value of a is defined as a_c. Then from (22a), the value of a_c is defined as follows:

$$a_c = \frac{b^2}{4 - (\sec(0.5\alpha\pi))^2}. \tag{23}$$

Traditionally, poles are used to determine the system stability. Consequently, it is necessary to prove the proposed analysis by comparing it with the singularities movement of the system. For fixed values of the fractional order α and the parameters b and c, as the value of a increases the system singularities move toward the stable region and the system becomes more stable as shown in Fig. 14a. Due to the symmetry of the transfer function, the effect of the parameter b on the system singularities and hence the stability is similar to the effect of a as depicted in Fig. 14b. On the other hand, as the value of c increases, the system singularities move toward the unstable region as shown

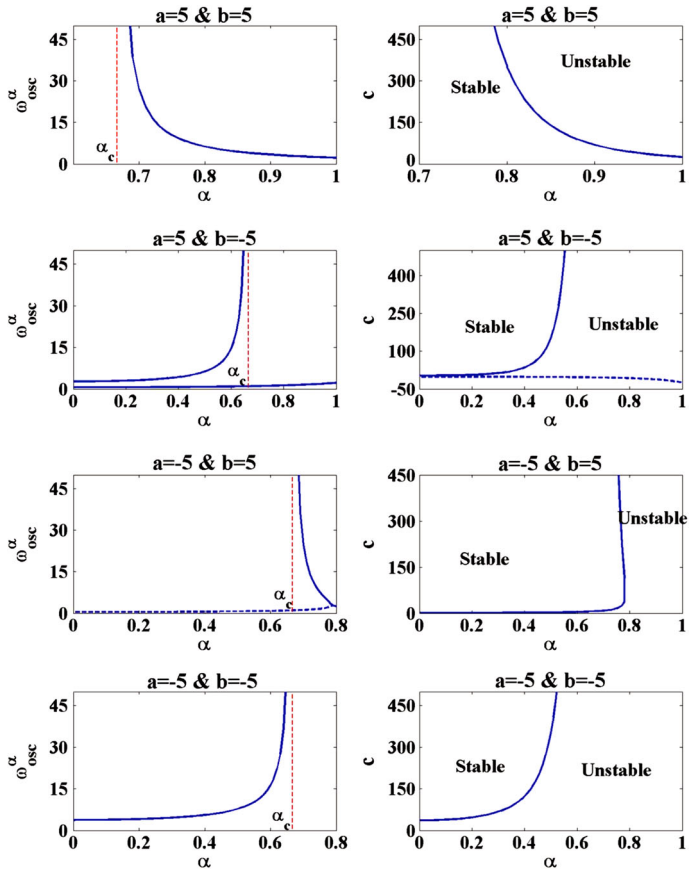

Fig. 12 Change in the oscillation frequency ($\omega_{\text{osc}}^{\alpha}$) and the stability contour with α at different values of a and b

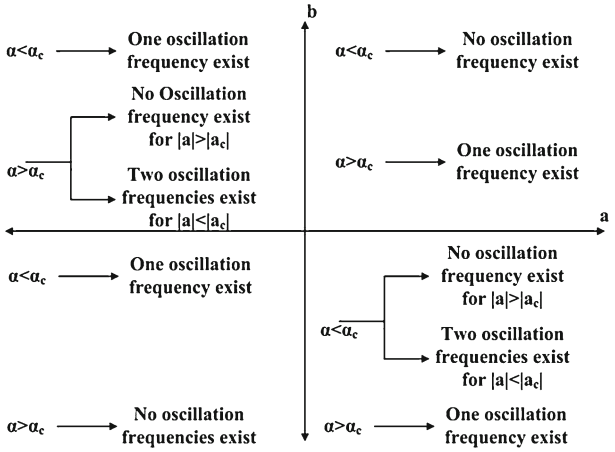

Fig. 13 Summary of the effect of a and α on the oscillation frequency ω_{osc}

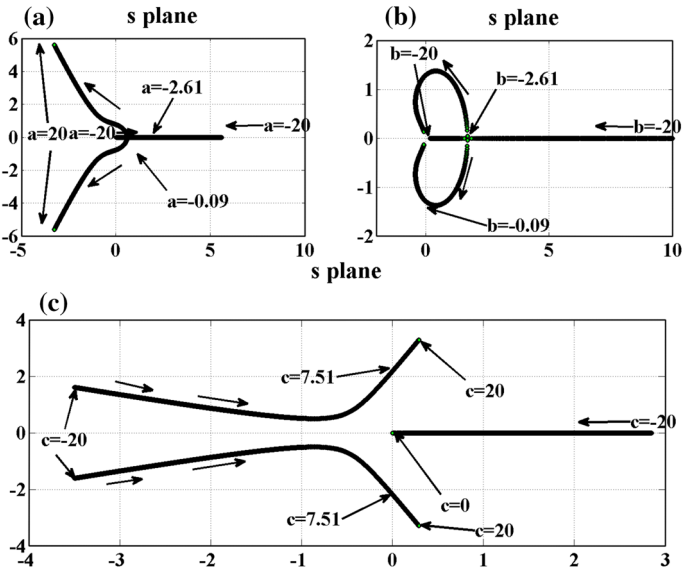

Fig. 14 Singularities movement with respect to a, b, and c for $\alpha = 0.8$, **a** $b = 1$ and $c = 1$, **b** $a = 1$ and $c = 1$, and **c** $a = b = 1$

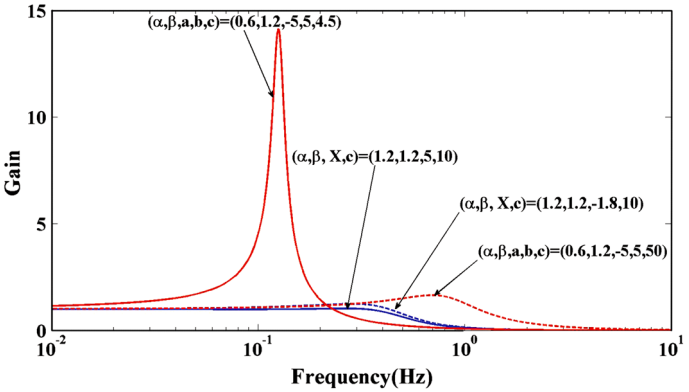

Fig. 15 Numerical simulation for the fractional order filter at different cases of the fractional orders

in Fig. 14c because $\alpha > \alpha_c$ as expected before. Then, the poles movement transfer function parameters matches with previous analysis. Finally, the work presented in this subsection can be generalized for any value of k.

Using the proposed stability analysis and the fractional order SK filter design method proposed in [41], numerical and experimental work for fractional order SK filter is presented to prove the reliability of the proposed analysis. For equal orders ($\alpha = \beta = 1.2$) and for $c = 10$, then from Fig. 11 for the filter to be stable the value of $X > -1.9$. The numerical analysis for the cases of $(\alpha, X) = (1.2, -1.8), (1.2, 5)$ is depicted in Fig. 15. The damping for the case of $X = -1.8$ is greater than the

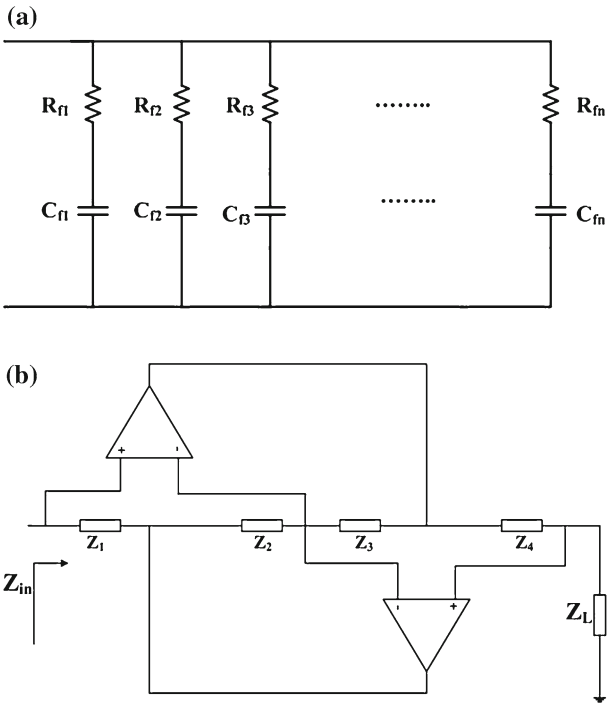

Fig. 16 **a** Equivalent RC tree circuit of the fractional order element of any order[18], and **b** The GIC circuit used to simulate fractional order element with order greater than unity [5]

case of the case of $X = 5$ because in the first case, the value of X is very close to the stability contour. Thus, for the filter to be stable without damping, the value of X should be far away from the stability contour as mentioned before. On the other hand, two SK filters of dependent orders with $k = 2$ are illustrated in Fig. 15 with the orders $(\alpha, \beta) = (0.6, 1.2)$ and $(a, b) = (-5, 5)$. In this case, for the filter to be stable and from Fig. 12, the value of $c > 4$. As shown in Fig. 15, the damping for the case of $c = 4.5$ is greater than the damping in the case of $c = 50$ because as expected. Finally, the relations tabulated in Table 3 are used to obtain the circuit components values. To study the fractional order filter experimentally, an equivalent RC circuit for the fractional order element of order less than unity based on the finite element approximation is illustrated in Fig. 16a [18]. The values of the resistances and capacitors of the equivalent circuit composed of fractional order capacitor with $Y_{\mathrm{F}} = s^{\alpha} C_{\mathrm{F}}$ are given by the following relations [18]:

$$R_{\mathrm{fn}} = \left[\frac{Y_F(\alpha) \sin(\alpha\pi)}{\pi} \sigma_n^{\alpha} \Delta(\ln(\sigma)) \right]^{-1}, \tag{24a}$$

$$C_{\mathrm{fn}} = \frac{Y_F(\alpha) \sin(\alpha\pi)}{\pi} \sigma_n^{\alpha-1} \Delta(\ln(\sigma)), \tag{24b}$$

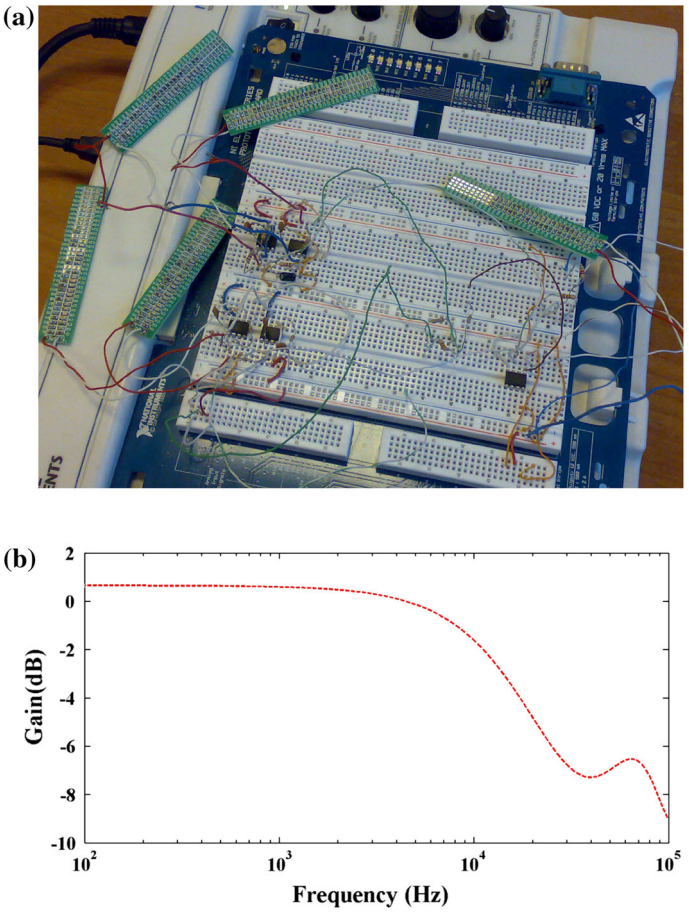

Fig. 17 **a** Photo of the practical fractional Sallen–Key filter. **b** Experimental results of the fractional Sallen–Key filter

where Y_F is the admittance value, σ is the relaxation rate corresponding to the pole of the nth branch, and $\Delta(\ln \sigma) = \ln \sigma_{n+1} - \sigma_n$ is the pole interval taken in a logarithmic scale. On the other hand, to obtain a fractional order element of order greater than unity, the generalized impedance converter (GIC) illustrated in Fig. 16b can be used [38]. Then, the practical fractional order Sallen–Key filter of the order $(\alpha, \beta, c) = (0.6, 1.2, 50)$ is implemented as shown in Fig. 17a by using the kit of NI ELVIS II from national instruments for measuring the outputs, the op-amp TL082, and the equivalent circuit of the fractional order element. As shown in Fig. 17b, the measured data after using the basic fitting techniques of the 7th order are very close to the numerical analysis. Consequently, the stability contours introduce a very easy way to design stable filters by choosing the value of the transfer function parameters inside the stable region. Then, the relations listed in Table 3 are used to calculate the circuit components value.

6 Conclusion

In this paper, the analysis of the singularities of the fractional order systems is proposed. The effect of the transfer function parameters on the number of poles is also presented. Then, stability contours for the fractional order Sallen–Key and KHN filter are presented to test the filter stability. Actually, it is found that these stability contours are more efficient than the system poles for the stability test because it is more flexible for the design process. Good results are obtained from the numerical and circuit simulations using the proposed stability contours.

References

1. A. Acharya, S. Das, I. Pan, S. Das, Extending the concept of analog butterworth filter for fractional order systems. Signal Process. **94**, 409–420 (2014)
2. R.P. Agarwal, D. O'Regan, *Ordinary and Partial Differential Equations: With Special Functions, Fourier Series, and Boundary Value Problems* (Springer, New York, 2009)
3. R. Alikhani, F. Bahrami, Global solutions for nonlinear fuzzy fractional integral and integrodifferential equations. Commun. Nonlinear Sci. Numer. Simul. **18**(8), 2007–2017 (2013)
4. H. Bateman, A. Erdélyi, W. Magnus, F. Oberhettinger, F.G. Tricomi, *Higher Transcendental Functions, vol. 2* (McGraw-Hill, New York, 1953)
5. B. Bhattacharyya, W.B. Mikhael, A. Antoniou, Design of rc-active networks using generalized-immittance converters. J. Frankl. Inst. **297**(1), 45–58 (1974). doi:10.1016/0016-0032(74). 90137–9
6. R. Caponetto, *Fractional Order Systems: Modeling and Control Applications, vol. 72* (World Scientific Publishing Company, Singapore, 2010)
7. S. Das, Application of generalized fractional calculus in electrical circuit analysis, in *Functional Fractional Calculus for System Identification and Controls*, (Springer, Berlin, 2008), pp. 157–180
8. A.S. Elwakil, Fractional-order circuits and systems: an emerging interdisciplinary research area. IEEE Circuits Syst. Mag. **10**(4), 40–50 (2010)
9. P. Fanghella, Fractional-order control of a micrometric linear axis. J. Control Sci. Eng. (2013)
10. R.H. Fox, J.W. Milnor et al., Singularities of 2-spheres in 4-space and cobordism of knots. Osaka J. Math. **3**(2), 257–267 (1966)
11. T.J. Freeborn, B. Maundy, A.S. Elwakil, Field programmable analogue array implementation of fractional step filters. IET Circuits Devices Syst. **4**(6), 514–524 (2010)
12. T.J. Freeborn, B. Maundy, A.S. Elwakil, Fractional step analog filter design, in *Analog/RF and Mixed-Signal Circuit Systematic Design*, ed. by M. Fakhfakh, E. Tlelo-Cuautle, R. Castro-Lopez. Lecture Notes in Electrical Engineering, vol. 233 (Springer, Berlin, 2013), pp. 243–267
13. L. Galeone, R. Garrappa, Explicit methods for fractional differential equations and their stability properties. J. Comput. Appl. Math. **228**(2), 548–560 (2009)
14. L.T. Grujić, Non-lyapunov stability analysis of large-scale systems on time-varying sets. Int. J. Control **21**(3), 401–415 (1975). doi:10.1080/00207177508921999
15. L.T. Grujić, Practical stability with settling time on composite systems. Automatika (Yug), Ljubljana pp. 1–11 (1975)
16. H.J. Haubold, A.M. Mathai, R.K. Saxena, Mittag-leffler functions and their applications. J. Appl. Math. **235**(5), 1311–1316 (2011)
17. A. Hegazi, E. Ahmed, A. Matouk, On Chaos control and synchronization of the commensurate fractional order liu system. Commun. Nonlinear Sci. Numer. Simul. **18**(5), 1193–1202 (2013)
18. M.S. Hirano, Y. Miura, Y.F. Saito, K. Saito, Simulation of fractal immittance by analog circuits: an approach to the optimized circuits. IEICE Trans. Fundam. Electron. Commun. Comput. Sci. **82**(8), 1627–1635 (1999)
19. T. Kaczorek, New stability tests of positive standard and fractional linear systems. Circuits Syst. **2**(4), 261–268 (2011)
20. M.P. Lazarevi, Finite time stability analysis of pd fractional control of robotic time-delay systems. Mech. Res. Commun. **33**(2), 269–279 (2006)

21. M.P. Lazarevi, A.M. Spasi, Finite-time stability analysis of fractional order time-delay systems: Gronwalls approach. Math. Comput. Modelling **49**(34), 475–481 (2009)
22. K. Li, Delay-dependent stability analysis for impulsive BAM neural networks with time-varying delays. Comput. Math. Appl. **56**(8), 2088–2099 (2008)
23. H. Li, Y. Luo, Y. Chen, A fractional order proportional and derivative (FOPD) motion controller: tuning rule and experiments. IEEE Trans. Control Syst. Technol. **18**(2), 516–520 (2010)
24. K.S. Miller, B. Ross, *An Introduction to the Fractional Calculus and Fractional Differential Equations* (Wiley, New York, 1993)
25. G. Mittag-Leffler, Sur la nouvelle fonction $E_\alpha(x)$. CR Acad. Sci. Paris **137**, 554–558 (1903)
26. K.B. Oldham, J. Spanier, *The Fractional Calculus, vol. 1047* (Academic Press, New York, 1974)
27. G. Peng, Synchronization of fractional order chaotic systems. Phys. Lett. A **363**(56), 426–432 (2007)
28. I. Podlubny, *Fractional Differential Equations: An Introduction to Fractional Derivatives, Fractional Differential Equations, to Methods of their Solution and Some of their Applications*, vol. 198. Access Online via Elsevier (1998)
29. A.G. Radwan, Stability analysis of the fractional-order $RL_\beta C_\alpha$ circuit. J. Fract. Calc. Appl. **3**(1), 1–15 (2012)
30. A.G. Radwan, A.S. Elwakil, A.M. Soliman, Fractional-order sinusoidal oscillators: design procedure and practical examples. IEEE Trans. Circuits Syst. I **55**(7), 2051–2063 (2008)
31. A.G. Radwan, A.S. Elwakil, A.M. Soliman, On the generalization of second-order filters to the fractional-order domain. J. Circuits Syst. Comput. **18**(02), 361–386 (2009)
32. A.G. Radwan, K. Moaddy, S. Momani, Stability and non-standard finite difference method of the generalized chuas circuit. Comput. Math. Appl. **62**(3), 961–970 (2011)
33. A.G. Radwan, K.N. Salama, Fractional-order RC and RL circuits. Circuits Syst. Signal Process. **31**(6), 1901–1915 (2012)
34. A.G. Radwan, A. Shamim, K.N. Salama, Theory of fractional order elements based impedance matching networks. IEEE Microwav. Wirel. Compon. Lett. **21**(3), 120–122 (2011)
35. A.G. Radwan, A.M. Soliman, A.S. Elwakil, A. Sedeek, On the stability of linear systems with fractional-order elements. Chaos Solitons Fractals **40**(5), 2317–2328 (2009)
36. D. Saha, D. Mondal, S. Sen, Effect of initialization on a class of fractional order systems: experimental verification and dependence on nature of past history and system parameters. Circuits Syst. Signal Process. **32**(4), 1501–1522 (2013)
37. R. Sallen, E. Key, A practical method of designing rc active filters. IRE Trans. Circuit Theory **2**(1), 74–85 (1955)
38. A.S. Sedra, P.O. Brackett, *Filter Theory and Design: Active and Passive* (Matrix Publishers, Portland, 1978)
39. A. Soltan, A.G. Radwan, A.M. Soliman, Butterworth passive filter in the fractional-order, in *2011 International Conference on Microelectronics (ICM)*, (IEEE, 2011) pp. 1–5
40. A. Soltan, A.G. Radwan, A.M. Soliman, Fractional order filter with two fractional elements of dependant orders. Microelectron. J. **43**(11), 818–827 (2012)
41. A. Soltan, A.G. Radwan, A.M. Soliman, Measurement fractional order Sallen–Key filters. Int. J. Electr. Electron. Sci. Eng. **7**(12), 2–6 (2013)
42. A. Soltan, A. Radwan, A. Soliman, CCII based KHN fractional order filter, in *2013 IEEE 56th International Midwest Symposium on Circuits and Systems (MWSCAS)* (2013), pp. 197–200
43. A. Soltan, A.G. Radwan, A.M. Soliman, CCII based fractional filters of different orders. J. Adv. Res. **5**(2), 157–164 (2014)
44. M.P. Tripathi, V.K. Baranwal, R.K. Pandey, O.P. Singh, A new numerical algorithm to solve fractional differential equations based on operational matrix of generalized hat functions. Commun. Nonlinear Sci. Numer. Simul. **18**(6), 1327–1340 (2013)
45. X. Zhang, L. Liu, Y. Wu, The uniqueness of positive solution for a singular fractional differential system involving derivatives. Commun. Nonlinear Sci. Numer. Simul. **18**(6), 1400–1409 (2013)